

Removal of Hexavalent Chromium Cr (VI) From an Aqueous Solution by an Industrial Waste from the Steelworks of the Algerian Steel Complex

Hamrouni Achraf^{1*}, Fiala Hichem^{2,3}, Ali Ahmed Atef^{2,4}, Boutaleb Yassira², Hattab Zhour^{2,*}, Berredjem Yamina³, Rebani Nacer², Guerfi Kamel².

¹Mines Metallurgy Materials Laboratory L3M National Hight school of Mines and Metallurgy, Amar Laskri, B.P.233, W129, Sidi Amar, R.P. Annaba 23000 Algeria.

²Department of Chemistry Lab of Water Treatment and Valorization of Industrial Wastes, Faculty of Science Badji-Mokhtar University, B.P.12, Annaba 23000, Algeria.

³Department of Chemistry Science and Technology Laboratory of Water and Environment, and Technology, Faculty of Science, Mohammed Cherif Messadia University, Souk Ahras 41000, Algeria.

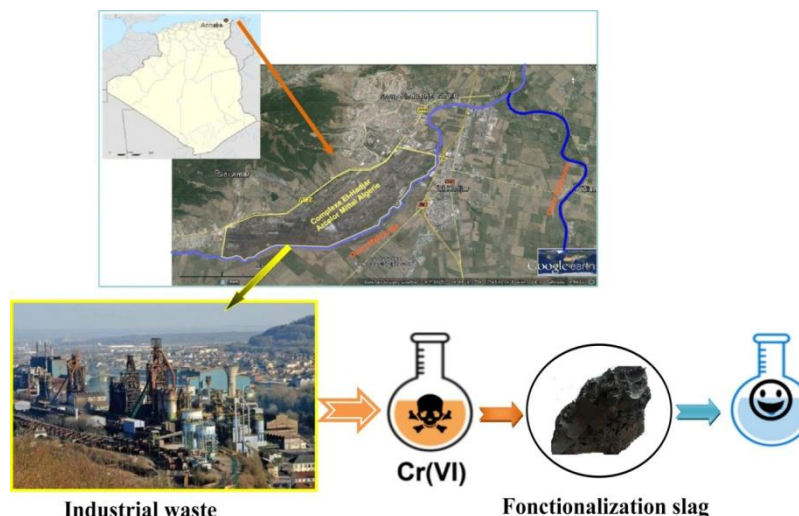
⁴Department of Process Engineering Science and Technology Laboratoire Physics of Matter and Radiation, Mohammed Cherif Messadia University, Souk Ahras 41000, Algeria.

1*achraf.hamrouni@ensmm-annaba.dz

2*zoumourouda20012000@yahoo.fr

ABSTRACT

Algeria has developed a dense Industrial network, concentrating polluting and water and energy consuming sectors. Slag, a waste product of the SIDER steel complex (Annaba, Algeria), was used as an adsorbent for the removal of hexavalent chromium from artificially contaminated aqueous solutions. The experiments were carried out in static regime. The determined best parameters influencing the adsorption such as mass of adsorbant, initial concentration, stirring speed, temperature, and pH, which allowed to reach a significant efficiency rate equal to 99% were as follow: Cr(VI) concentration of 10 ppm, pH 1, contact time at equilibrium 30 min and a temperature of 40°C. Modeling of the experimental data showed that the pseudo-second order model describes the adsorption kinetics in an adequate way. Also, the adsorption isotherms are in agreement with the Freundlich model. Furthermore, the thermodynamic analysis revealed that the studied adsorption process is a favorable, endothermic, and spontaneous phenomenon.



Keywords: Slag; Chromium-hexavalent; Waste; Adsorption, Modeling.

Introduction

Water is the source of life and the most important factor in achieving sustainable economic and social development. Therefore, its pollution is a critical problem for all mankind. Heavy metals are a major source of water pollution resulting from several industrial activities, including tanneries, synthetic dyes and leather industries [1, 2], and metal surface treatment [3]. Among these metals, the chromium which is in nature under several forms depending on its degree of oxidation. Of the two most stable forms, trivalent Cr and hexavalent Cr, Cr(VI) represents the greatest threat to the environment and human health, given its high toxicity and carcinogenic potential [4-6]. Several remediation processes have been developed to remove Cr(VI) from industrial effluents with the objective of environmental protection and possible reuse of water. These include chemical precipitation [7], ion exchange [8], nanoparticles [9, 10], reverse osmosis [11], electrocoagulation [12], membrane separation [13], and photocatalysis [14]. However, most of these technologies are expensive, especially when applied to high flow rate effluents. Adsorption technique [15] has been proven to be effective in the treatment of aqueous effluents especially in the removal of heavy metals from water [16], but most conventional adsorption systems use activated carbon despite its high production cost and difficulties in regeneration [17]. Recently, many researchers have focused on cheaper adsorbents for adsorption tests. The objective of this work is the valorization of an industrial waste, the slag resulting from the operation of refining at the level of an electric steel plant of the steel complex Sider El-hadjar (Annaba, Algeria) in order to eliminate Cr(VI) in aqueous solution by adsorption in static regime. This will enable us to achieve a triple objective: to reduce pollution, to recover a waste product and to recycle water. To this end, we will study the parameters that have an influence on the adsorption equilibrium (pH, mass, agitation speed, temperatures, concentration) in order to determine the optimal conditions. A modeling of the adsorption isotherms and a thermodynamic study will also be carried out to understand the nature of the reaction mechanisms involved in the present adsorption phenomenon.

1. MATERIALS AND METHOD

1.1. Chemical products

All chemicals used in the adsorption tests such as hydrogen chloride (HCl), sodium hydroxide (NaOH), sulfuric acid (H₂SO₄), 1,5-diphenylcarbazine, and potassium dichromate (K₂Cr₂O₇) were purchased from Sigma-Aldrich-Fluka (Saint-Quentin, Fallavier, France).

1.2. Preparation of adsorbent

The material used was a slag from the refining operation at an electric steel mill of Sider El-hadjar (Annaba, Algeria). The sample was crushed and then sieved, only the particles with sizes between 50-125µm were used.

1.3. Caractérisations of the adsorbent

The chemical composition of the slag was determined using X-ray fluorescence spectroscopy (ARL Thermo Scientific Perform X). The surface functional groups of the sample were identified by Fourier Transform Infrared spectroscopy (FT-IR) analysis using IR⁻¹ affinity in combination with a single ATR reflection. The morphology of the sample was determined using a scanning electron microscope (SEM) (Quanta 200 FEI) combined with scatter X-ray. The crystal structure of the material was characterized by X-ray diffraction (XRD) (Philips model PW1710) using K α

copper radiation ($\lambda = 1.5460 \text{ \AA}$) with 40 kV, 40 mA, a scan speed of 0.01 min^{-1} and an angle 2θ between 0 and 90.

1.4. Adsorption kinetics of Cr (VI).

The adsorption kinetics of Cr(VI) under the different operating conditions (initial concentration, stirring speed, pH, and temperature) was carried out in a static regime. A sample mass of 12.5 g.L^{-1} was mixed with a Cr(VI) solution. The suspensions were stirred with a mechanical stirrer. Over time, a constant volume of supernatant was taken and determined after centrifugation using a UV-Vis spectrophotometer (TECHCOMP 8500) at a wavelength of $\lambda_{max} = 545 \text{ nm}$. The removal efficiency of Cr(VI) is calculated by equation (1)[18]:

$$R (\%) = \frac{C_0 - C_e}{C_0} \quad (1)$$

Where, R is the yield (%); C_0 and C_e are the initial and equilibrium concentration (mg.L^{-1}) respectively

The quantities of Cr (VI) adsorbed were calculated using equation (2) [18].

$$q_e = \frac{V(C_0 - C_e)}{m} \quad (2)$$

Where q_e (mg.g^{-1}) is the equilibrium adsorption capacity; C_0 and C_e are the initial and equilibrium concentration (mg.L^{-1}) respectively; V (L) is the volume of the solution; m (g) is the mass of the adsorbent.

1.5. Adsorption isotherm for Cr (VI)

The adsorption isotherms were carried out at different concentrations, under the optimal conditions established in the kinetic study ($m = 12.5 \text{ g.L}^{-1}$, pH = 1, T = 25°C , constant stirring speed 150 rev / min, contact time 30 minutes). The suspensions, after stirring, were centrifuged and the supernatant was then analyzed.

2. Results and Discussion:

2.2 . Material Characterisation

2.2.1 Chemical Composition of Slag

The chemical composition of the slag was carried out by X-ray fluorescence. The results obtained are presented in Table 1.

Table 1. Chemical composition of slag.

Composition%	Fe	CaO	SiO ₂	MgO	Al ₂ O ₃	MnO	ZnO	P ₂ O ₅
Scorie	12,43	32,30	31,44	7,70	2,52	16,64	0,12	0,36

According to this analysis, the slag consists of a mixture of oxides rich in (CaO, SiO₂), a low content of (MnO, Fe, MgO), and a poor content of (ZnO, P₂O₅, Al₂O₃).

2.2.2 X-ray Analysis

3 The X-ray diffraction pattern of the slag (Fig.1) shows that the sample is crystalline, with a

very intense SiO_2 peak at about $2\theta = 26.46^\circ$, (JSPD 96-900-9667), peaks representing calcium oxide CaO (JSPD 96-101-1328) Lime and Calcite CaCO_3 (JSPD 96-901-6707) as well as MnO Manganosite (JSPD 96-900-6670) due to its chemical composition rich in $(\text{CaO-SiO}_2\text{-MnO})$ (fig.5). We can see that calcites in their different forms are the main compounds of slag.

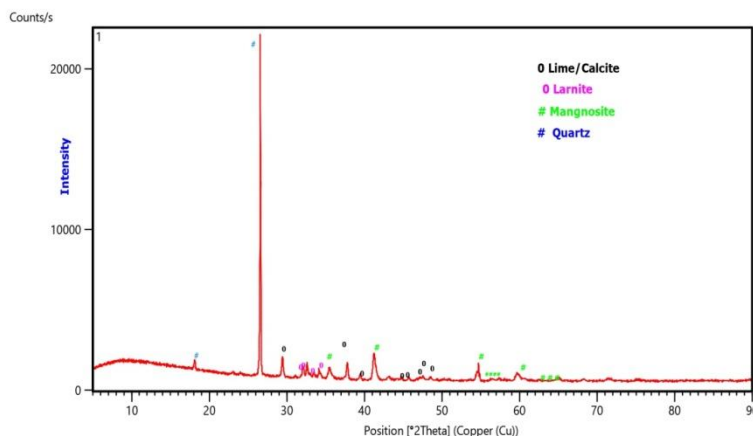


Figure.1: X-ray diffraction pattern of slag

2.2.3. IR-TF Analysis

The IR-FT spectrum of the slag (Fig. 2) shows different peaks which are attributed to various functional groups and bands. Absorption bands at $3355\text{-}3738\text{ cm}^{-1}$ and $1508\text{-}1648\text{ cm}^{-1}$ reflect the presence elongation and deformation vibrations of the O-H and H-O-H bonds of the adsorbed water molecules respectively[19,20]. Calcite phase C-O is further confirmed by presence of prominent peak at 2361.85 . The absorption peaks appearing at 669 and 868 cm^{-1} are attributed to the elongation of the Al-O and Si-O bonds respectively [21].

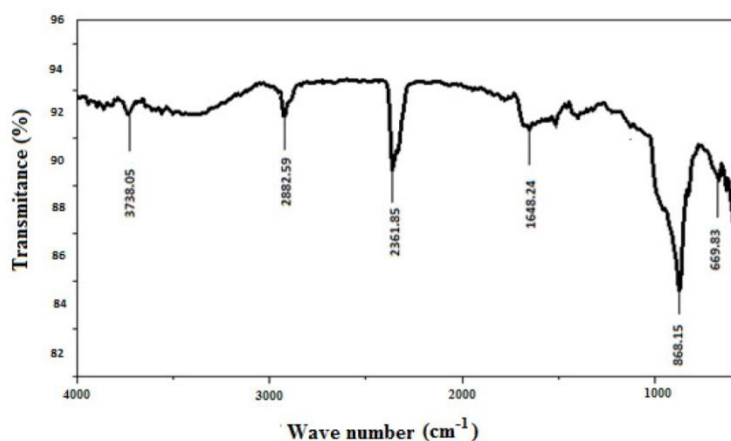


Figure.2: IR-FT of the slag.

2.2.4. SEM Analysis

The morphological structure of the slag before and after adsorption is shown in (fig.3) at different magnifications. The (SEM) images clearly show that the wall of a slag has a large number of small holes; these holes promote the transport of chemical species in all directions through the slag, which may be suitable for the retention of pollutants.

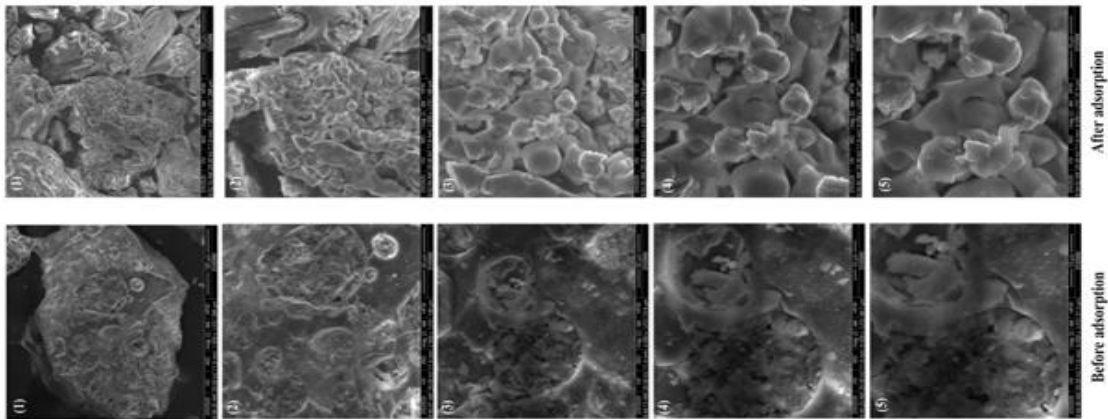


Figure. 3 SEM images before and after adsorption.

2.2.5. EDX Analyses

The atomic and mass percentage presented in (fig. 4 (a) and (b))indicate that the slag is of mineral nature. Fig. 4(b) shows the EDX profile of the slag after adsorption. We notice the appearance of a Cr(VI) peak, which confirms the fixation of Cr(VI) on the slag.

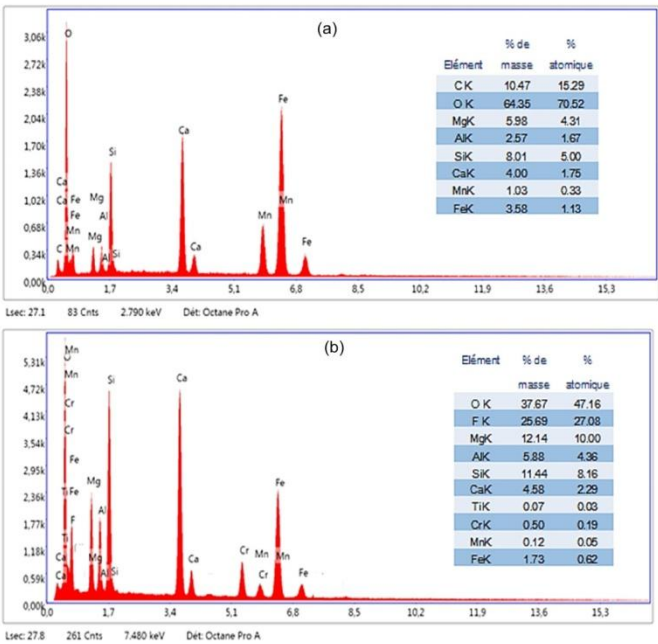


Figure .4 EDX profile of the slag (a) before and (b) after adsorption

2.3. Kinetic Study
2.3.1. pH effect

The initial pH of the solution is an important parameter that must be considered in any adsorption study. The effect of this factor on the retention rate of Cr(VI) was analyzed over a pH range of 1 to 6. According to the literature the predominant forms of Cr(VI) in aqueous solution are $\text{H}_2\text{Cr}_2\text{O}_7$ at $\text{pH} < 1$, HCrO_4^- at $1 < \text{pH} < 6$, and CrO_4^{2-} at $\text{pH} > 6$ [22].

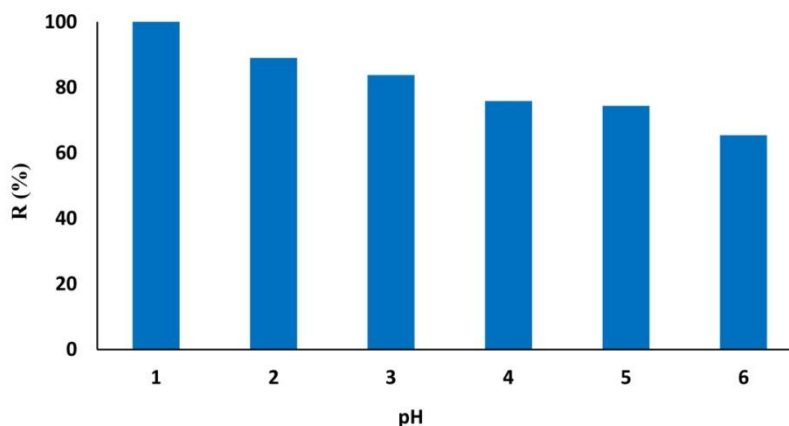


Figure.5 Effect of pH on slag adsorption yield for the removal of Cr (VI) ($C_0=10\text{mg. L}^{-1}$, $\text{pH}=1$, $m=12.5\text{g L}^{-1}$, $V_a=150\text{rpm}$).

The results, presented in Fig.5, showed that the maximum percentage removal of Cr(VI) occurs at $\text{pH} = 1$, for an initial concentration of 10 mg/L. The removal rate decreases with increasing pH of the solution, this behaviour is explained by the fact that at $\text{pH}=1$ the surface of the adsorbent can be strongly protonated with H^+ ions, resulting in the development of a positive electric charge on the surface of the support, this charge presents an electrostatic attraction of the HCrO_4^- ions and favours the adsorption of Cr (VI), which increases the percentage of removal [23]. This behavior is also explained by the fact that at $\text{pH} = 1$, the oxides that constitute the slag tend to form aquacomplexes that cause an increase in the positive charge density on the surface of the slag (a positively charged surface) and consequently an increase in Cr(VI) adsorption. The active functional groups on the surface of the slag might be the deprotonated (Si-O-) sites since the main constituent of the slag is SiO_2 .

2.3.2 Mass Effect

Equilibrium time plays a key role in the design of wastewater treatment systems [23]. In order to determine the necessary amount of slag corresponding to maximum removal, suspensions of 20 mL of 10 ppm Cr (VI) solution were prepared in Pyrex tubes, to which masses of slag ranging from 0.1g to 0.5g were added.

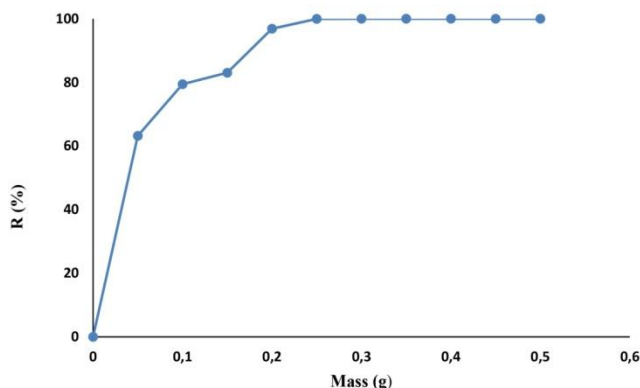


Figure.6 Effect of adsorbent mass on Cr(VI) removal by slag ($C_0=10\text{mg. L}^{-1}$, $\text{pH}=1$, $V_a= 50 \text{ rpm}$) The results show that the percentage of Cr(VI) removal increases with increasing mass. Above a mass of 0.25g, the rate tends to stabilize and the appearance of a saturation plateau (Fig.6). This is attributed to the increase in the number of active sorption sites.

2.3.3 Effect of stirring speed

The speed of stirring is also considered as an important parameter in the adsorption process [24]. In order to study its effect on the retention process, three agitation speeds were considered: 50,100,150 rpm.

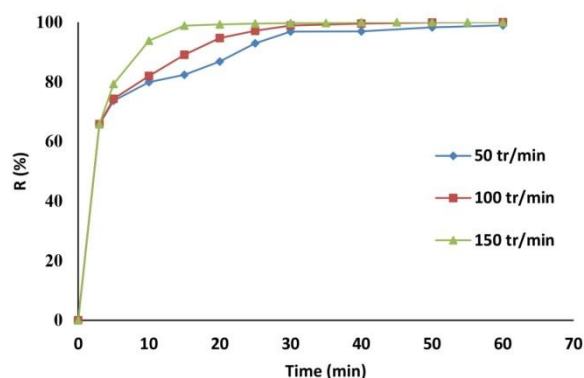


Figure.7 Effect of stirring speed on Cr (VI) removal by slag ($C_0=10\text{mg. L}^{-1}$, $\text{pH}=1$, $m=12.5\text{g. L}^{-1}$)

From (fig.7), it can be seen that high stirring speed increases the retention process. However, a very high stirring speed improves the mass transfer of Cr(VI) molecules to the solid support.

2.3.4 Effect of concentration

To study the influence of the initial hexavalent chromium concentration on the adsorption process, tests were carried out by varying the concentrations from 10 to 30mg.L^{-1} . The other parameters were kept constant.

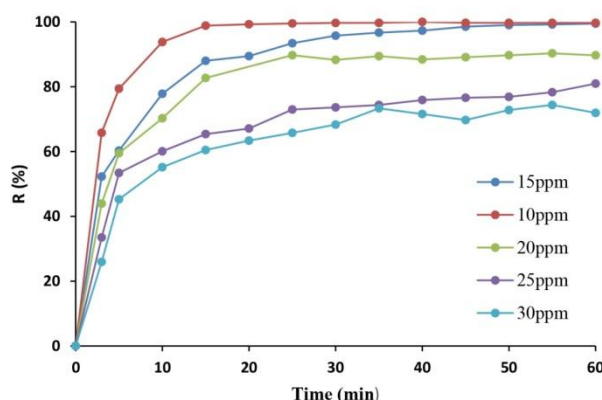


Figure. 8 Effect of initial concentration of Cr(VI) adsorption on slag (pH=1, m=12.5mg. L⁻¹, Va=150rpm)

According to (fig.8), the retention efficiency decreases with increasing concentration; this is probably due to the saturation of the surface adsorbent sites by chromium (VI).

2.3.5 Influence of temperature

In order to study the influence of temperature on the retention of Cr (VI), three different temperatures were chosen 20, 30 and 40°C. Figure.9 shows that an increase in temperature from 20 to 40 °C induces an increase in the removal rate of Cr (VI) on the slag.

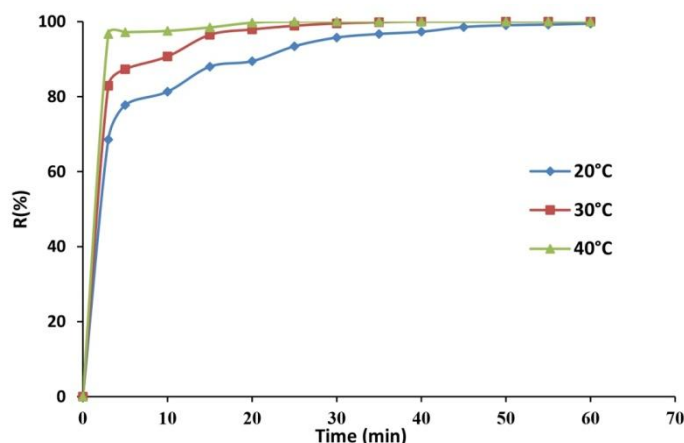


Figure.9 Effect of temperature on Cr(VI) removal by slag (C0=15mg. L⁻¹, pH=1, Va=150 rpm)

Figure.9 show that an increase in temperature from 20 to 40 ° C induces an increase in the rate of removal of Cr (VI) from the slag. This indicates that the displacement process is endothermic which may be the result of increased mobility of Cr (VI) ions with increasing temperature [25] and may be due to increased thermal energy of the adsorbent species when the temperature was increased [26].

2.3.6 Contact time effect

The kinetic study of Cr (VI) adsorption on slag requires the knowledge of contact times, in order to reach the equilibrium between the adsorbate and the adsorbent. For this purpose, we followed the adsorption kinetics for an initial concentration of 10 mg.L^{-1} , with a mass of the slag of 12.5 g.L^{-1} .

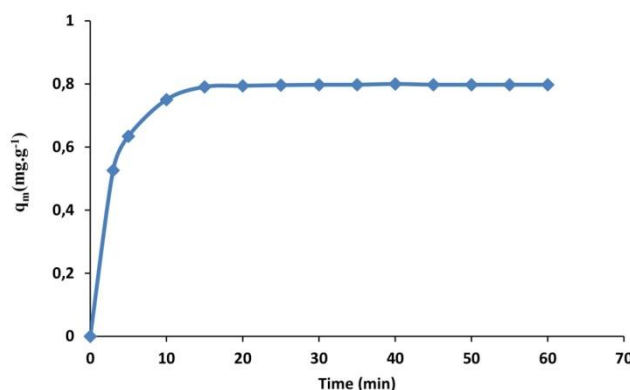


Figure.10 Adsorption kinetics of Cr (VI) on the slag ($m = 12.5 \text{ g/L}$, $C = 10 \text{ mg.L}^{-1}$, $\text{pH} = 1$, and $T = 20^\circ\text{C}$).

According to the shape of the curve (fig.10), we notice a rapid fixation of the pollutant and equilibrium is reached after 15 minutes. The speed of adsorption can be explained by the fact that at the start of adsorption the number of active sites available on the surface of the adsorbent material is much greater than the number of sites remaining after a certain time [27]. At this level there is a pseudo-equilibrium between the rate of adsorption and desorption, the adsorption becomes relatively slower giving the impression of equilibrium. In all of the adsorption tests, we opted for a time of 30 minutes to ensure that the balance between the different phases was established.

2.4 Adsorption kinetics

Several kinetic models are developed to highlight the essential parameters of the adsorption kinetics. The adsorption of Cr(VI) on slag has been modeled using the pseudo-first order Equation (3) and pseudo-second order [28] Equation (4):

$$\ln(q_e - q_t) = \ln q_e - k_1 t \quad (3)$$

$$\frac{t}{q_t} = \frac{1}{k_2 q_e^2} + \frac{t}{q_e} \quad (4)$$

Where, t : contact time; k_1 : adsorption rate constant of pseudo-first order kinetics; k_2 : adsorption rate constant of pseudo-second order kinetics; q_t and q_e : adsorption capacities at time t and equilibrium respectively.

Table 2. Summary of the results of the different kinetic models.

Modèles		$q_e \text{ (exp)} (\text{mg} \cdot \text{g}^{-1})$	
PPO	$q_e \text{ (cal)} (\text{mg} \cdot \text{g}^{-1})$	0.5363	
	K_1	0.2450	
	R^2	0,976	0,7941
PSO	$q_e \text{ (cal)} (\text{mg} \cdot \text{g}^{-1})$	0.8084	
	K_2	2.0539	
	R^2	0.999	

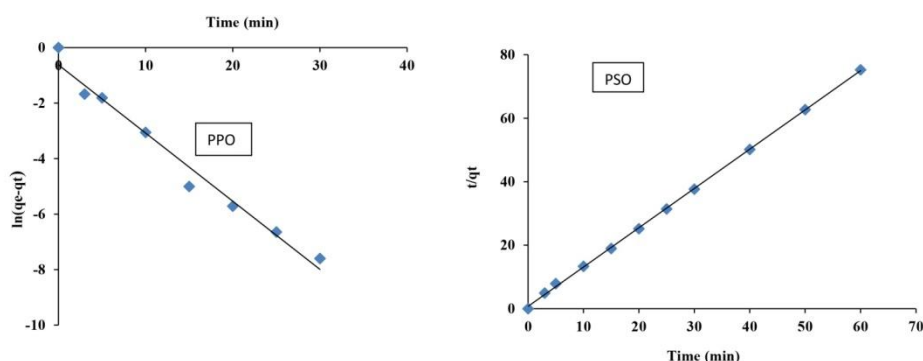


Figure.11 Linear regression of various kinetic models (a) PFO and (b) PSO ($m=12.5 \text{ g} \cdot \text{L}^{-1}$, $C=10 \text{ mg} \cdot \text{L}^{-1}$, $\text{pH}=1$ and $T=20^\circ\text{C}$).

The results of the kinetics of our adsorbent are shown by fig 11(a),(b) and gathered in Table 2. According to the value of the two correlation coefficients (R^2) the PSO kinetic model is the most convenient to describe the adsorption process of Cr (VI) on the slag. Furthermore, the theoretically calculated ($q_{e,cal}$) by this model are in good agreement with those of the experiment ($q_{e,exp}$).

2.5 Adsorption isotherm

Establishing adsorption isotherms allows us to calculate the maximum amount adsorbed by the solid and also to identify the type of adsorption. According to Gille's classification [29], the experimental results show an increase in adsorption with an increase in the adsorbate concentration indicating that the isotherm is type H (Fig. 12). The amount of chromium adsorbed at equilibrium is given by the following equation:

$$q_e = \frac{V(C_0 - C_e)}{m} \quad (5)$$

Where (mg.g^{-1}) is the equilibrium adsorption capacity; C_0 and C_e are the initial and equilibrium concentrations (mg.L^{-1}) respectively; V (L) is the volume of the solution; $m(g)$ is the mass of the adsorbent.

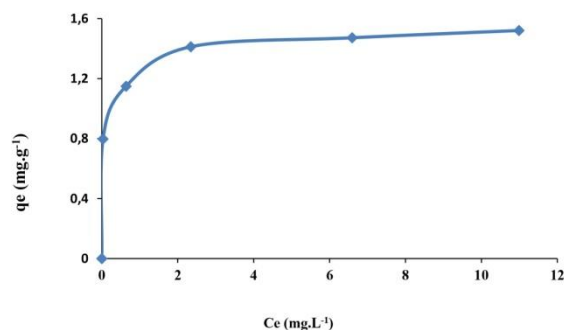


Figure.12 Adsorption isotherm of Cr (VI) on slag ($m=12.5\text{g.L}^{-1}$, $C=10\text{mg L}^{-1}$, $\text{pH}= 1$ and $T=20^\circ\text{C}$)

2.6 Langmuir Isotherm

The Langmuir model assumes that metal ion absorption occurs on a homogeneous surface by monolayer adsorption without any interaction between the adsorbed ions [30].

The Langmuir equation in linear form is expressed by equation. (6):

$$\frac{1}{q_e} = \frac{1}{q_m} + \frac{1}{K_L \times q_m} \times \frac{1}{C_e} \quad (6)$$

Where C_0 is the initial concentration of metal ions (mg.L^{-1}).

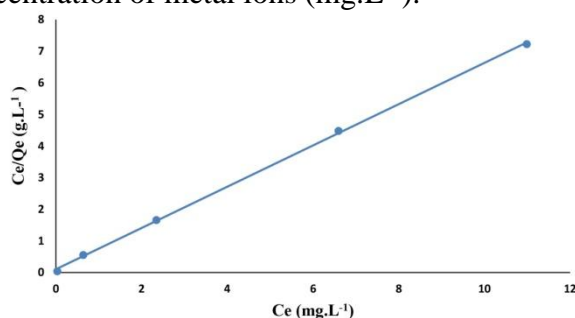


Figure.13 Langmuir linearization for Cr(VI) adsorption on slag.

Table 3. Calculated values of the separation factor R_L

C_0	10	15	20	25	30
R_L	0,01550575	0,01039087	0,00781345	0,006260543	0,005222569

From (fig.13), we notice that the linearization of adsorption isotherm of Cr(VI) on slag is satisfactory, with a value of calculated adsorption quantity equal to the experimental adsorption quantity and good correlation coefficient. We can say that the Langmuir model is adequate for a

good description of this adsorption. The found values of $0 < R_L < 1$ indicate a very favorable adsorption for the slag.

2.7 Freundlich Isotherm

The Freundlich equation is an empirical model based on heterogeneous adsorption on independent sites. The linear form of the Freundlich equation (7) is as follows [31]:

$$\ln q_e = \ln K_F + \frac{1}{n} \ln C_e \quad (7)$$

K_F and n are the Freundlich constants. The values of K_F and n were determined from the intercept and slope of the line graph of $\ln q_e$ versus $\ln C_e$ in (fig.14), respectively, and the results are presented in Table.4.

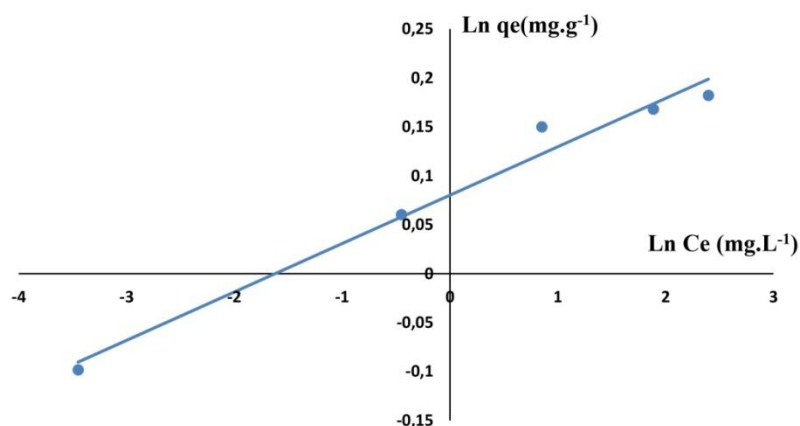


Figure.14 Freundlich linearization for Cr(VI) on slag

The intensity parameter, $1/n$ indicates the deviation of the adsorption isotherm from linearity. When $1/n=0$, the adsorption is linear, i.e. the sites are homogeneous and there is no interaction between the adsorbed species. When $1/n < 1$, the adsorption is favorable, the adsorption capacity increases and new sites appear. When $1/n > 1$ adsorption is not favorable, the adsorption bonds become weak and the adsorption capacity decreases [32]. From the obtained results we can see that the ratio $1/n$ is less than 1, so the Freundlich isotherm is favorable for the adsorption of Cr on the slag. A value of n between 1 and 10 represents a good adsorption [33].

2.8 Temkin isotherm

Adsorbent-adsorbate interactions are a crucial factor for this isotherm. By lifting the ultimate low and high concentration values, the model assumes that the heat of adsorption (as a function of

temperature) of all molecules in the layer would decrease linearly rather than logarithmically in the blanket [34]. Temkin isotherm has generally been represented by the following equations(8) [35,36]:

$$q_e = B \ln A_T + B \ln C_e \quad (8)$$

where $B = \frac{RT}{b_T}$, b_T (J.mol⁻¹) is the heat of adsorption, A_T is the equilibrium binding constant Lg^{-1} , RT is the adsorption constant $J\ mol^{-1}$, R is the universal gas constant $8.314\ J\ mol^{-1}\ K^{-1}$, T is the absolute value of temperature [298 K]. The constant parameters of the Temkin isotherm were determined from the linear curve of (q_e) versus $\ln(C_e)$ fig.15.

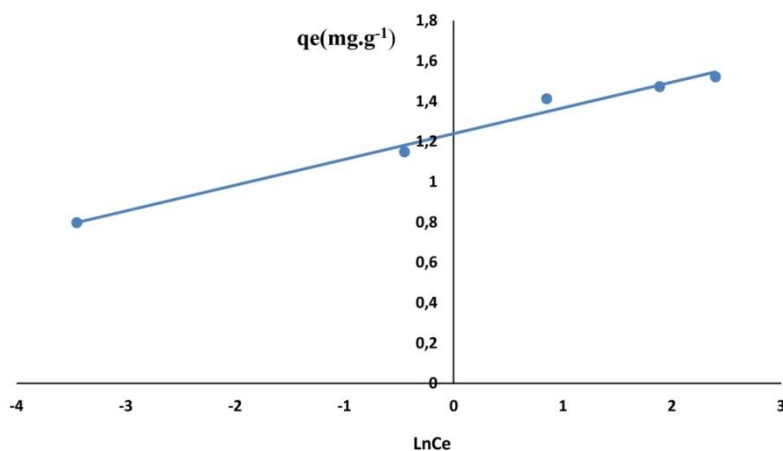


Figure.15 Temkin linearization for Cr(VI) on slag

Table 4. Langmuir, Freundlich and Temkin isotherm constants for Cr(VI) adsorption on slag.

Model		
Langmuir	$q_{m(exp)}(mg.g^{-1})$	1,5209
	$q_{m(cal)}(mg.g^{-1})$	1,5320
	$K_L(g^{-1})$	6,3492
	R^2	0,9995
Freundlich	$1/n$	0,0494
	$K_F^{(mg\ l^{-1/n} L^{1/n} g^{-1})}$	1,0835
	R^2	0,9791

Temkin	$\Delta Q(KJ/mol)$	29,1874769
	$A(L.g^{-1})$	16220,8578
	B_1	0,1278
	R^2	0,9837

As presented in Table 4, the maximum monolayer coverage capacity (qm) of the Langmuir isotherm model was found to be 3.06 mg. g⁻¹, K_L (Langmuir isotherm constant) is 0.078 (L mg⁻¹). The R_L values for the adsorption of Cr (VI) on slag are in the range (0.719 to 0.125) (Table 3). The value of R_L is lower than the unit, it indicates that the equilibrium sorption is favorable and the high value of the correlation coefficient R² (0.984) proves that the sorption data fit well with the Langmuir Isotherm model and then come the Temkin and Freundlich models. Therefore, it can be understood that, Langmuir and Temkin isotherms are the most suitable models for the sorbate-sorbent system. The variation of adsorption energy is positive with the adsorbent used, hence the adsorption of chromium by the slag is endothermic, which confirms the results obtained during the study of the temperature effect.

2.9 Determination of thermodynamic parameters

The effect of temperature on the adsorption of hexavalent chromium was studied in order to obtain the relevant thermodynamic parameters. The free energy of adsorption (ΔG°), entropy (ΔS°), and enthalpy change (ΔH°) in the adsorption process are related to the Vant Hoff equations [37]:

$$\Delta G^\circ = -RT \ln K_C \quad (9)$$

$$\ln K_C = \frac{\Delta H^\circ}{RT} - \frac{\Delta S^\circ}{R} \quad (10)$$

$$K_C = \frac{C_{Ae}}{C_{Se}} \quad (11)$$

Where $\ln K_C$ [38] is the equilibrium constant, C_{Ae} is the amount of adsorbate on the adsorbent per volume of solution (L) at equilibrium (mg L⁻¹), C_{Se} is the equilibrium concentration of adsorbate in the aqueous solution (mg.L⁻¹), R is the gas constant 8.314 JK⁻¹ mol⁻¹, and T is the temperature (K). The values of (ΔH°) and (ΔS°) were obtained from the slope and intersection of the $\ln K_C$ against 1/T curve according to (fig.16).

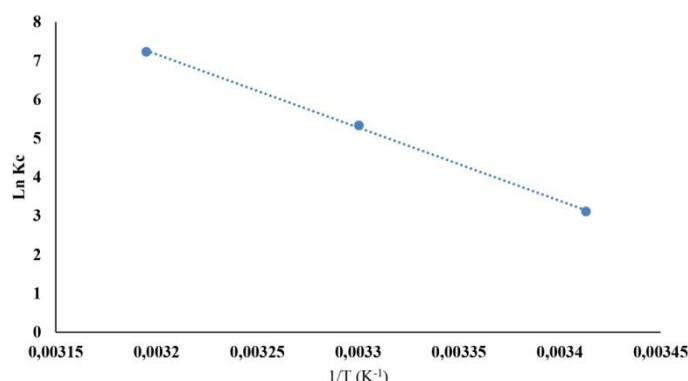


Figure.16 Determination of the enthalpy and entropy of adsorption of Cr(VI) on slag.

Table 5. Thermodynamic parameters of adsorption of chromium (VI) ions by slag at different temperatures.

T(K)	ΔH° (KJ/mol)	ΔS° (KJ/mol)	ΔG° (KJ/mol)
293			-7.58
303	157.017	0.562	-12.98
313			-17.61

From the results, it is observed that the free energy values for the different temperatures are below zero ($\Delta G^\circ < 0$) [39], which proves that the removal process of Cr(VI) ions is spontaneous. This shows that high temperatures, in the studied range, favor adsorption.

The positive value of the enthalpy variation ($\Delta H^\circ > 0$) indicates again that the adsorption of Cr (VI) by the slag is an endothermic process [40]. The positive value of entropy ($\Delta S^\circ > 0$) indicates the increase of the disorder at the adsorbate-adsorbent interface during the adsorption of chromium on the surface [41-44].

3. Conclusion

This work showed that slag could be used for the removal of Cr(VI) from aqueous effluents. The study of the influence of the parameters (pH, mass, initial concentration, agitation speed and temperature), allowed the determination of the optimal conditions.

The adsorption kinetics is best described by the pseudo-second order model. According to the Gilles classification, the experimental results showed that the isotherm shape is H-type. The adsorption isotherms of our adsorbent obey to the Langmuir model indicating a homogeneous monolayer adsorption. The study of the thermodynamic parameters (ΔH° , ΔG° and ΔS°) showed that the fixation process of Cr(VI) ions on the slag is endothermic and spontaneous

Acknowledgement

The authors gratefully acknowledge financial support from the Algerian Ministry of Higher Education and Scientific Research.

References

- [1] Barenhart, J., “Occurrences, (1997) *uses, and properties of chromium*. *Regulat. Toxicol. Pharmacol.*, 26, 3-7.
- [2] M.H. Dehghani, M.M. Taher, A.K. Bajpai, B. Heibati, I. Tyagi, M. Asif, S. Agarwal, V.K. Gupta, (2015), *Removal of noxious Cr (VI) ions using single-walled carbon nanotubes and multi-walled carbon nanotubes*, *Chem. Eng. J.*, 279 344–352.
- [3] B.J. Alloway, *Heavy metals in soils.*, 1995, 2nd ed., Blackis Academic and Professional, London,.
- [4] Shanker, A., C., Cervantes, H., Loza-Tavera et S., Avudainayagam. (2005) *Chromium toxicity in plants*. *Environ. Inter.* , 31, 739-753.
- [5] P.K. Tyagi, (2017), *Study of potentiality of coal fly ash for the removal of Cr(VI) from industrial wastewater: equilibrium and kinetic studies*, *Int. J. Eng. Technol. Sci. Res.*, 4 836–843.
- [6] J. Ali, L. Wang, H. Waseem, R. Djellabi, N.A. Oladoja, G. Pan, (2019), *FeS@rGONanocomposites as electrocatalysts for enhanced chromium removal and clean energy generation by microbial fuel cell*, *Chem. Eng. J.* 123335.
- [7] M.M. Matlock, B.S. Howerton, D.A. Atwood, (2002) ,*Chemical precipitation of heavy metals from acid mine drainage*, *Water Res.*, 36 4757–4764.
- [8] X. Li, P.G. Green, C. Seidel, C. Gorman, J.L. Darby, (2016), *Chromium removal from strong base anion exchange waste brines*, *J. Am. Water Works Assoc.*, 108 E247–E255.
- [9] Zaid Hamid Mahmoud. The Magnetic Properties of Alpha Phase for Iron Oxide NPs that Prepared from its Salt by Novel Photolysis Method. *Journal of Chemical and Pharmaceutical Research*, 2017, 9(8):29-33
- [10] S. Rangabhashiyam, N. Selvaraju, B. Raj Mohan, P.K. Muhammed Anzil, K.D. Amith, E.R. Ushakumary, (2016), *Hydrous cerium oxide nanoparticles impregnated enteromorpha sp. for the removal of hexavalent chromium from aqueous solutions*, *J. Environ. Eng. (United States)*, 142 1–9.
- [11] Padilla, A.P. et E.L., Tavani, (1999)., “*Treatment of an industrial effluent by reverse osmosis*”. *Desalination*, 129, 219-226
- [12] K. Industry, W. Water, (2015), *Efficiency of removing chromium from plating industry wastewater using the electrocoagulation method*, *Q. Int. Arch. Heal. Sci.*, 2 83–87.
- [13] P.A. Vinodhini, P.N. Sudha, (2017), *Removal of heavy metal chromium from tannery effluent using ultrafiltration membrane*, *Text. Cloth. Sustain*, 2 5.
- [14] R. Li, D. Hu, K. Hu, H. Deng, M. Zhang, A. Wang, R. Qiu, K. Yan, (2019), *Coupling adsorption-photocatalytic reduction of Cr (VI) by metal-free N-doped carbon*, *Sci. Total Environ.* 704 135284.
- [15] Zaid Hamid Mahmoud, Marwa Sabbar Falih, Omaila Emad Khalaf, Mohammed Alwan Farhan, Farah Kefah Ali. *Photosynthesis of AgBr Doping TiO₂ Nanoparticles and degradation of reactive red 120 dye*. *J Adv Pharm Edu Res* 2018;8(4):51-55.
- [16] J. Geng, Y. Yin, Q. Liang, Z. Zhu, H. Luo, (2019), *Polyethyleneimine cross-linked graphene oxide for removing hazardous hexavalent chromium: Adsorption performance and mechanism*, *Chem. Eng. J.* 361 1497–1510.
- [17] Momina, M. Shahadat, S. Isamil, (2018), *Regeneration performance of clay-based adsorbents for the removal of industrial dyes: A review*, *RSC Adv.* 8 24571–24587.
- [18] M Kavitha, Z. H. Mahmoud, Kakarla Hari Kishore, AM Petrov, Aleksandr Lekomtsev, Pavel

- Iliushin, Angelina Olegovna Zekiy, Mohammad Salmani. application of Steinberg Model for Vibration Lifetime Evaluation of Sn-Ag-Cu-Based Solder Joints in Power Semiconductors. IEEE Transactions on Components, Packaging and Manufacturing Technology. 2021; 11(3):444-450.
- [19] U. Rattanasak, P. Chindaprasirt, (2009), *Influence of NaOH solution on the synthesis of fly ash geopolymer*, Miner. Eng. 22 1073–1078.
- [20] D. Panias, I.P. Giannopoulou, T. Perraki, (2007), *Effect of synthesis parameters on the mechanical properties of fly ash-based geopolymers*, Colloids Surfaces A Physicochem. Eng. Asp. 301
- [21] Z. Yunsheng, S. Wei, L. Zongjin, (2010) , *Composition design and microstructural characterization of calcined kaolin-based geopolymer cement*, Appl. Clay Sci. 47 271–275.
- [22] Marzouk Trifi I., 2012. *Étude de l'élimination du chrome VI par adsorption sur l'alumine activée par dialyse ionique croisée*, Thèse de doctorat, Université de Tunis El-Manar.
- [23] Sanchez-Polo M., J. Rivera-Ultrilla 2002. *Adsorbent-adsorbate interaction in the adsorption of Cd (II) and Hg (II) on ozonized activated carbon*. Environ. Sci. Technol., 36, 3850–3854.
- [24] Nandi, Barun Kumar, Goswami, Amit, Kumar Purkait, Mihir, 2009b. *Adsorption characteristics of brilliant green dye on kaolin*. J. Hazard Mater. 161 (1), 387–395. 246–254.
- [25] Arvind Kumar, Hara Mohan Jena, 2017, *Adsorption of Cr(VI) from aqueous solution by prepared high surface area activated carbon from Fox nutshell by chemical activation with H₃PO₄* Journal of Environmental Chemical Engineering. 5, 2032-2041.
- [26] S.K. Lagergren, (1898) , *About the theory of so-called adsorption of soluble substances*, Sven. Vetenskapsakad. Handlingar. 24 1–3.
- [27] Benguella B., yacouta- Nour A., 2009. *Elimination des colorants acides en solution aqueuse par la bentonite et le kaolin*. C.R. Chimie 12 : 762-771.
- [28] Hector R. Guzmán-Carrillo, Alejandro Manzano-Ramírez, Ines Garcia Lodeiro, and Ana Fernández Jiménez, (2020) *ZnO Nanoparticles for Photocatalytic Application in Alkali-Activated Materials* Molecules, 25, 5519
- [29] Y.S. Ho, G. McKay, (1999), *Pseudo-second order model for sorption processes*, Process Biochem. 34 451–465.
- [30] C.H. Giles, T.H. MacEwan, S.N. Nakhwa, *System of classification of solution adsorption isotherms and its use in diagnosis of adsorption of mechanisms and in measurements of specific surface area of solids*, J. Chem. Soc., 10 (n.d.) 3973–3993.
- [31] G. McKay, M.S. Otterburn, A.G. Sweeney, (1980) , *The removal of colour from effluent using various adsorbents-III*. Silica: Rate processes, Water Res. 14 15–20.
- [32] E. Malkoc, Y. Nuhoglu, (2007) , *Potential of tea factory waste for chromium(VI) removal from aqueous solutions: Thermodynamic and kinetic studies*, Sep. Purif. Technol. 54 291–298.
- [33] H. Peng,., Shang, Q., Chen, R. et al. (2020), *Step-Adsorption of Vanadium (V) and Chromium (VI) in the Leaching Solution with Melamine* Sci Rep 10, 6326.
- [34] A.. Dada, (2012), *Langmuir, Freundlich, Temkin and Dubinin–Radushkevich Isotherms Studies of Equilibrium Sorption of Zn 2+ Unto Phosphoric Acid Modified Rice Husk*, IOSR J. Appl. Chem. 3 38–45.
- [35] M.I. Temkin, 1979, *The Kinetics of Some Industrial Heterogeneous Catalytic Reactions*,.

- [36] R.R. Krishni, K.Y. Foo, B.H. Hameed, (2014), Adsorption of methylene blue onto papaya leaves: comparison of linear and nonlinear isotherm analysis, *Desal. Water Treat.*, 52 6712–6719
- [37] K. Kayalvizhi, K. Vijayaraghavan, M. Velan, (2015), *Biosorption of Cr(VI) using a novel microalga Rhizoclonium hookeri: equilibrium, kinetics and thermodynamic studies*, *Desalin. Water Treat.* 56 194–203.
- [38] A.M. Donia, A.A. Atia, H. El-Boraey, D.H. Mabrouk, Uptake, (2006) , *studies of copper(II) on glycidyl methacrylate chelating resin containing Fe₂O₃ particles*, *Sep. Purif. Technol.* 49 64–70.
- [39] Z. Aksu, Ü. Açikel, E. Kabasakal, S. Tezer, (2002), *Equilibrium modelling of individual and simultaneous biosorption of chromium(VI) and nickel(II) onto dried activated sludge*, *Water Res.* 36 3063–3073.
- [40] Guendouz S., 2017. *Elimination of Cr (VI) in aqueous solution by tamazert kaolin and its dosage in complex form*, PhD thesis, Badji Mokhtar-Annaba University, Algeria
- [41] N. Öztürk, D. Kavak, *Adsorption of boron from aqueous solutions using fly ash: Batch and column studies*, (2005) , *J. Hazard. Mater.* 127 81–88.
- [42] E.K. Guechi, O. Hamdaoui, (2016), *Evaluation of potato peel as a novel adsorbent for the removal of Cu(II) from aqueous solutions: equilibrium, kinetic, and thermodynamic studies*, *Desalin. Water Treat.* 57 10677–10688.
- [43] C. Djelloul, O. Hamdaoui, (2014), *Removal of cationic dye from aqueous solution using melon peel as nonconventional low-cost sorbent*, *Desalin. Water Treat.* 52 7701–7710.
- [44] S. Nawaz, H.N. Bhatti, T.H. Bokhari, S. Sadaf, (2014) , *Removal of Novacron black dye from aqueous solutions using low cost agricultural waste: Batch and fixed bed study*, *Sci. Iran.* 21 2066–207.